

# Lasing properties of polymerized chiral nematic Bragg onion microlasers

MATJAŽ HUMAR,<sup>1,2,3,\*</sup> FUMITO ARAOKA,<sup>4</sup> HIDEO TAKEZOE,<sup>5</sup> AND IGOR MUŠEVIČ<sup>1,2</sup>

<sup>1</sup>*J. Stefan Institute, Jamova 39, SI-1000, Ljubljana, Slovenia*

<sup>2</sup>*Faculty of Mathematics and Physics, University of Ljubljana, Jadranska 19, SI-1000, Ljubljana, Slovenia*

<sup>3</sup>*Wellman Center for Photomedicine, Harvard Medical School, Massachusetts General Hospital, 65 Landsdowne St. UP-5, Cambridge, Massachusetts 02139, USA*

<sup>4</sup>*RIKEN Center for Emergent Matter Science, 2-1 Hirosawa, Wako, Saitama 351-0198, Japan*

<sup>5</sup>*Toyota Physical and Chemical Research Institute, 41-1 Yokomichi, Nagakute, Aichi 480-1192, Japan*

\*[matjaz.humar@ijs.si](mailto:matjaz.humar@ijs.si)

**Abstract:** Dye doped photocurable cholesteric liquid crystal was used to produce solid Bragg onion omnidirectional lasers. The lasers were produced by dispersing and polymerizing chiral nematic LC with parallel surface anchoring of LC molecules at the interface, extracted and transferred into another medium. Lasing characteristics were studied in carrier medium with different refractive index. The lasing in spherical cholesteric liquid crystal was attributed to two mechanisms, photonic bandedge lasing and lasing of whispering-gallery modes. The latter can be suppressed by using a higher index carrier fluid to prevent total internal reflection on the interface of the spheres. Pulse-to-pulse stability and threshold characteristics were also studied and compared to non-polymerized lasers. The polymerization process greatly increases the lasing stability.

© 2016 Optical Society of America

**OCIS codes:** (140.3945) Microcavities; (160.1585) Chiral media; (160.3710) Liquid crystals; (160.5293) Photonic bandgap materials; (230.1480) Bragg reflectors.

## References and links

1. I. Muševič, "Liquid-crystal micro-photonics," *Liq. Cryst. Rev.* **4**, 1-34 (2016).
2. H. Coles and S. Morris, "Liquid-crystal lasers," *Nat. Photonics* **4**, 676–685 (2010).
3. V. I. Kopp, B. Fan, H. K. M. Vithana, and A. Z. Genack, "Low-threshold lasing at the edge of a photonic stop band in cholesteric liquid crystals," *Opt. Lett.* **23**, 1707–1709 (1998).
4. M. Ozaki, M. Kasano, D. Ganzke, W. Hasse, and K. Yoshino, "Mirrorless lasing in a dye-doped ferroelectric liquid crystal," *Adv. Mater.* **14**, 306–309 (2002).
5. W. Cao, A. Munoz, P. Palfy-Muhoray, and B. Taheri, "Lasing in a three-dimensional photonic crystal of the liquid crystal blue phase II," *Nat. Mater.* **1**, 111–113 (2002).
6. H. Kikuchi, M. Yokota, Y. Hisakado, H. Yang, and T. Kajiyama, "Polymer-stabilized liquid crystal blue phases," *Nat. Mater.* **1**, 64–68 (2002).
7. T. Ohta, M. H. Song, Y. Tsunoda, T. Nagata, K.-C. Shin, F. Araoka, Y. Takanishi, K. Ishikawa, J. Watanabe, S. Nishimura, T. Toyooka, H. Takezoe, "Monodomain film formation and lasing in dye-doped polymer cholesteric liquid crystals," *Jpn. J. Appl. Phys.* **43**, 6142–6144 (2004).
8. H. Finkelmann, S. T. Kim, A. Munoz, P. Palfy-Muhoray, and B. Taheri, "Tunable mirrorless lasing in cholesteric liquid crystalline elastomers," *Adv. Mater.* **13**, 1069–1072 (2001).
9. T. Manabe, K. Sonoyama, Y. Takanishi, K. Ishikawa, and H. Takezoe, "Toward practical application of cholesteric liquid crystals to tunable lasers," *J. Mater. Chem.* **18**, 3040–3043 (2008).
10. S. M. Morris, A. D. Ford, M. N. Pivnenko, and H. J. Coles, "The effects of reorientation on the emission properties of a photonic band edge liquid crystal laser," *J. Opt. A: Pure Appl. Opt.* **7**, 215 (2005).
11. F. Araoka, K.-C. Shin, Y. Takanishi, K. Ishikawa, H. Takezoe, Z. Zhu, and T. M. Swager, "How doping a cholesteric liquid crystal with polymeric dye improves an order parameter and makes possible low threshold lasing," *J. Appl. Phys.* **94**, 279–283 (2009).
12. J. Schmidtke, W. Stille, H. Finkelmann, and S. T. Kim, "Laser emission in a dye doped cholesteric polymer network," *Adv. Mater.* **14**, 746–749 (2002).
13. S. M. Jeong, N. Y. Ha, Y. Takanishi, K. Ishikawa, and H. Takezoe, "Defect mode lasing from a double-layered dye-doped polymer cholesteric liquid crystal films with a thin rubbed defect layer," *Appl. Phys. Lett.* **90**, 261108 (2007).

14. M. Humar, M. Ravnik, S. Pajk, and I. Muševič, "Electrically tunable liquid crystal optical microresonators," *Nat. Photonics* **3**, 595–600 (2009).
15. M. Humar and I. Muševič, "Surfactant sensing based on whispering-gallery-mode lasing in liquid-crystal microdroplets," *Opt. Express* **19**, 19836–19844 (2011).
16. M. Humar and I. Muševič, "3D microlasers from self-assembled cholesteric liquid-crystal microdroplets," *Opt. Express* **18**, 26995–27003 (2010).
17. P. J. W. Hands, D. J. Gardiner, S. M. Morris, C. Mowatt, T. D. Wilkinson, and H. J. Coles, "Band-edge and random lasing in paintable liquid crystal emulsions," *Appl. Phys. Lett.* **98**, 141102 (2011).
18. D. J. Gardiner, S. M. Morris, P. J. W. Hands, C. Mowatt, R. Rutledge, T. D. Wilkinson, and H. J. Coles, "Paintable band-edge liquid crystal lasers," *Opt. Express* **19**, 2432–2439 (2011).
19. G. Cipparrone, A. Mazzulla, A. Pane, R. J. Hernandez, and R. Bartolino, "Chiral self-assembled solid microspheres: a novel multifunctional microphotonic device," *Adv. Mater.* **23**, 5773 (2011).
20. I. Gourevich, L. M. Field, Z. Wei, C. Paquet, A. Petukhova, A. Alteheld, E. Kumacheva, J. J. Saarinen, and J. E. Sipe, "Polymer multilayer particles: a route to spherical dielectric resonators," *Macromolecules* **39**, 1449–1454 (2006).
21. Y. Xu, W. Liang, A. Yariv, J. G. Fleming, and S.-Y. Lin, "Modal analysis of Bragg onion resonators," *Opt. Lett.* **29**, 424–426 (2004).
22. M. G. Donato, J. Hernandez, A. Mazzulla, C. Provenzano, R. Saija, R. Sayed, S. Vasi, A. Magazzu, P. Pagliusi, R. Bartolino, P. G. Gucciardi, O. M. Marago, and G. Cipparrone, "Polarization-dependent optomechanics mediated by chiral microresonators," *Nat. Commun.* **5**, 3656 (2014).
23. R. J. Hernandez, A. Mazzulla, A. Pane, K. Volke-Sepúlveda, and G. Cipparrone, "Attractive-repulsive dynamics on light-responsive chiral microparticles induced by polarized tweezers," *Lab. Chip.* **7**, 459–467 (2013).
24. E. Brasselet, N. Murazawa, H. Misawa, and S. Juodkazis, "Optical vortices from liquid crystal droplets," *Phys. Rev. Lett.* **103**, 103903 (2009).
25. D. Seč, T. Porenta, M. Ravnik, and S. Žumer, "Geometrical frustration of chiral ordering in cholesteric droplets," *Soft Matter* **8**, 11982–11988 (2012).
26. G. Posnjak, S. Čopar, and I. Muševič, "Points, skyrmions and torons in chiral nematic droplets," *Sci. Rep.* **6**, 26361 (2016).
27. K.-C. Shin, F. Araoka, B. Park Y. Takahashi, K. Ishikawa, Z. Zhu, T. M. Swager, and H. Takezoe, "Advantages of highly ordered polymer-dyes for lasing in chiral nematic liquid crystals," *Jpn. J. Appl. Phys.* **43**, 631 (2004).

## 1. Introduction

The use of soft matter self-assembly to produce photonic microcomponents such as photonic crystals, diffractive elements, lasers and waveguides paves the way to novel micro optical systems, which are adaptive, biocompatible and scalable [1]. Liquid crystals (LCs) are in this regard especially useful because of high degree of self assembly, tunability and a large variety of different structures that can be assembled from different phases. Notably, chiral nematic liquid crystals exhibit spontaneous 1D helical organization with the period (pitch) in the visible wavelength range, which makes them 1D photonic crystals. When such a periodic liquid crystal is doped with a fluorescent dye, an optical gain is introduced into the 1D photonic crystal, which acts as a distributed feedback optical resonator. By pumping fluorescently labeled chiral nematic liquid crystal with an external source of light, lasing can be achieved along the direction of helical modulation [2]. Lasing was also demonstrated in different chiral liquid crystalline phases, such as chiral nematic liquid crystals (cholesteric liquid crystals, CLCs) [3], smectic chiral liquid crystals [4] and blue phase liquid crystals [5].

Wavelength of the laser emission from LC lasers is determined by its intrinsic periodicity and is tunable by external stimuli, such as electric field and temperature. When the stability of the laser is necessary, the tunability can be a drawback, therefore to stabilize the lasing, the LC molecules can be bound into a polymer network. By polymerization the internal LC structure can be frozen. The director configuration usually changes very little during polymerization. The order parameter sometimes increases or decreases a little, but not much. During the polymerization the internal structure can be manipulated by external factors such as surface anchoring, temperature and electric field. After the polymerization the LC will maintain the same structure even if the external stimuli are not present anymore, since the polymerized LC is not sensitive anymore to external stimuli. This can also be a drawback, since the system is not tunable anymore. Although partial polymerization can be used for stabilizing only the framework keeping the

switchability [6].

Lasing has been achieved in different polymer CLCs, such as polymer networks [7], elastomers [8] and photocurable LCs [9]. For lasing applications pump laser pulses with high peak power are usually used for excitation. The pump pulse locally increases the temperature and reorients the LC, in this way temporarily changing the optical properties of the LC introducing instabilities to the system [10]. Therefore CLC lasers usually work at low repetition rates in the range of hertz. It has been shown that the introduction of a polymeric dye into a cholesteric liquid crystal improves the order parameter reduces the lasing threshold [11]. The polymerization can stabilize the lasing, both the wavelength and the pulse-to-pulse energy. This is especially important in optical applications, since thermal fluctuations of the nematic director continuously changes the optical properties of the material. The lasing threshold may increase [9] or decrease [12] after polymerization, as the order parameter does. We should properly choose materials to improve the lasing characteristics. Besides the lasing action itself, polymer LCs provide us with additional merits; free-standing lasing sheet [13] and possible manipulation after polymerization, as will be described in this paper.

In most cases of lasing in LCs, a thin layer of the lasing medium is placed in between two centimeter size glass plates. To reduce the footprint of the laser, the LC can be formed into a micrometer sized droplet in an external carrier fluid or polymer. In the most simple case a tens-of-micrometer diameter droplet of a nematic liquid crystal can be used as the laser cavity and the refractive index of the outside medium is selected to be lower than the refractive index of the droplet. The light inside the droplet is therefore totally internally reflected at the interface and is trapped in the droplet. The resulting modes of circulation of light inside the droplet are called the Whispering-Gallery Modes (WGMs). In droplets of a nematic liquid crystal WGMs can be largely tuned by application of the electric field [14] and lasing can be achieved as well [15]. A droplet of a chiral nematic liquid crystal with parallel surface anchoring of LC molecules at the interface can also be used as a laser. In this case the axis of helical pitch is pointing radially from the center to the surface of the droplet, making an omnidirectional laser [16]. The CLC can be also encapsulated in a polymer matrix enabling directional emission without the need of alignment layers [17, 18]. The CLC droplet lasers can also be made from photocurable LCs, so that after the polymerization solid microlasers are formed [19]. Solid Bragg-onion cavities were also produced before by chemical synthesis [20] or by combining etching and chemical vapor deposition [21], but lasing has not been achieved in these structures. The polymerized chiral particles also exhibit very interesting optical properties which enable polarization-dependent optomechanics [19, 22, 23] and generation of optical vortices [24]. However, omnidirectional lasing, one of the most interesting application of polymerized CLC particles, has not been studied into detail. The lasing from CLC particles can arise from different resonant mechanisms, such as whispering-gallery modes and random lasing, not only from photonic band edge lasing. In addition, structural imperfections or dye bleaching could be induced during polymerization of the CLC microdroplet. The present paper addresses these questions by measuring spectral characteristics and lasing stability of polymerized CLC microdroplets.

## 2. Methods

For the preparation of the droplets two polymerizable cholesteric liquid crystals were used: RMS03-008 and RMS03-009 (Merck). A few percent of a non-polymerizable nematic liquid crystal ZLI-2293 (Merck) was added to the mixture to reduce the viscosity of the mixture and increase the pitch, so that the long wavelength edge of the photonic bandgap matched the maximum emission of the fluorescent dye. DCM dye (4-(dicyanomethylene)-2-methyl-6-(4-dimethylaminostyryl)-4H-pyran, Exciton) was used as the gain medium. The exact composition of the mixture was 34.0wt% of RMS03-008, 60.8wt% of RMS03-009, 4.1wt% of ZLI-2293 and 1.1wt% of DCM). The components were thoroughly mixed at 100 °C so that the mixture

was in the isotropic phase. After cooling to room temperature the mixture was centrifuged to remove any remaining undissolved solid particles. The final mixture had a cholesteric-to-isotropic phase transition of 85 °C. A few percent of the CLC mixture was introduced into glycerol, that was preheated to 60 °C. To produce the droplets the glycerol was vigorously mixed with the pipette tip for 10 s. Dispersing the CLC at higher temperature decreases its viscosity and enables efficient annihilation of the defects in single droplets, therefore creating droplets with perfect spherulite structure. The dispersion of droplets was introduced in between a microscope slide and a cover slip and sealed with an epoxy glue. The sample was then exposed for 5 minutes to UV (365 nm) with intensity of 400  $\mu\text{W}/\text{cm}^2$ . In the case we wanted to extract the polymerized CLC microlasers out of the glycerol, no cover slip was used. After the UV exposure the dispersion was dissolved in water and the polymerized particles were washed five times with deionized water using centrifugation to extract the particles. The polymerized CLC microlasers were dried at 50 °C for two hours. The final dry lasers could be mixed with any liquid. In our case we used immersion oil (Nikon) as a high index fluid ( $n = 1.52$ ).

To compare the lasing characteristics of the polymerized micro lasers with the non-polymerizable ones, a mixture of a commercial nematic liquid crystal MLC-7023 (Merck) with 25.5wt% S-811 chiral dopant and 0.2wt% fluorescent dye Nile red (7-diethylamino-3,4-benzophenoxazine-2-one, Sigma-Aldrich) was used [16].

Single polymerized droplets were observed under an inverted optical microscope. An actively Q-switched doubled Nd:YAG laser (Alphas, Pulselas-A-1064-500) with a pulse length of 1 ns and a maximum pulse energy of 10  $\mu\text{J}$  was focused by a 20 $\times$  objective to a waist diameter of  $\sim 100 \mu\text{m}$  illuminating the dispersed microlasers. The repetition rate of the laser pulses was typically 10 Hz. The laser uniformly illuminated a single CLC microdroplet and the fluorescent or lasing light produced by the droplet was analyzed by an imaging spectrometer (Andor, Shamrock SR-500i) with the resolution of 0.05 nm and an EM-CCD camera (Andor, Newton DU970N).

### 3. Results and discussion

By mixing CLC with glycerol, a dispersion of droplets with different sizes is produced (Fig. 1(a)). The droplets visually look exactly the same before and after the exposure to UV light. Smaller droplets look similar to the droplets made out of non-polymerizable CLC. They have a point defect in the center and a line defect that extends from the center to the surface of the droplet [25]. In droplets larger than  $\sim 30 \mu\text{m}$  the point defect may not be positioned exactly in the center of the droplet. Very larger droplets with diameters tens of micrometers usually contained many defects and did not have a regular internal structure. It was recently revealed by a fluorescent confocal polarizing microscopy that CLC droplets contain a variety of point defects, accompanied by metastable and smoothly twisted defect structures [26]. The reason for the irregular structure of larger droplets with many defects is the high viscosity of polymerizable LCs that prevents the annihilation of defects. Therefore, to decrease the viscosity, a small amount of non-polymerizable nematic LC ZLI-2293 was added to the mixture and the mixture was heated to just below the clearing point while mixing with glycerol. The droplets containing defect are not desirable, since they usually do not lase. However, if they lase, they emit laser light into an irregular pattern and wavelength.

When a single polymerized droplet embedded in glycerol was illuminated by the pulsed laser, a bright spot appeared in the center of the droplet and a bright ring was visible on the circumference (inset in Fig. 2), corresponding to Bragg lasing and lasing of WGMs, respectively. The spectrum of light emitted by the droplet (Fig. 2) contains several equally spaced spectral lines originating from WGMs lasing and an overlapping sharper peak at around 600 nm that matches to the 3D Bragg lasing. The Bragg lasing only takes place at the long wavelength edge of the photonic bandgap according to the Fermi's Golden rule [27]. Moreover, this edge at 600 nm is matched to the maximum emission of the fluorescent dye. In contrast the short wavelength

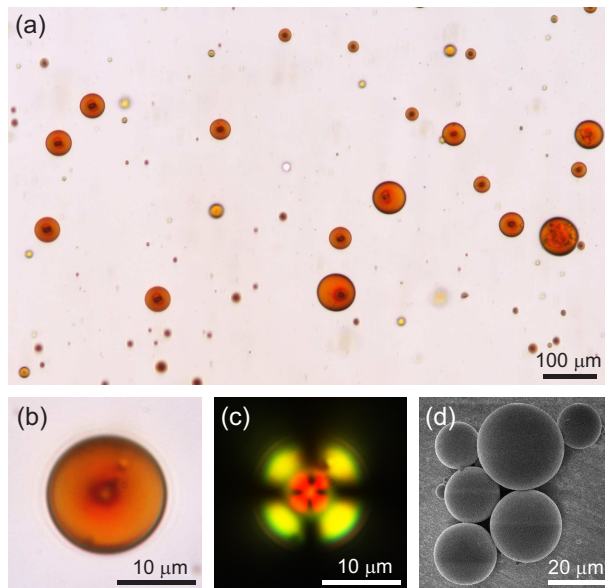


Fig. 1. (a) Dispersion of polymerized CLC droplets in glycerol. Their red color is due to DCM fluorescent dye. Larger droplets do not have a perfect spherulite structure and may contain several defects. (b) A single CLC droplet (15  $\mu\text{m}$ ) with a defect at the center and (c) the same droplet under crossed polarizers. (d) SEM image of a cluster of polymerized dried spheres.

edge at 520 nm is far from the maximum gain region of the dye (585 - 610 nm). The Bragg lasing linewidth is 0.2 nm, while the WGMs lasing linewidths are dependent on the microlaser diameter. For the microsphere in Fig. 2 the WGM linewidth is 0.9 nm.

To confirm that the spectral lines correspond to two kinds of modes, a spatially resolved spectrum was captured using an imaging spectrometer. The image of the droplet from the microscope was projected onto the plane of the spectrometer slit so that the center of the droplet was in the center of the slit (inset of Fig. 3). The collection area of the slit corresponds to a  $1 \mu\text{m} \times 60 \mu\text{m}$  rectangle on the sample. In the resulting spectrum (Fig. 3) a series of spectral lines are extending through the whole diameter of the droplet and they have much higher intensity at the edge of the droplet. These lines correspond to lasing of WGMs. A spectral peak at around 600 nm with high intensity is observed in the center of the droplet, clearly indicating that it corresponds to Bragg lasing. The WGM lasing is more pronounced when the polymerized CLC lasers are extracted from the glycerol and used in a lower refractive index medium such as water. Because of higher index contrast in water the WGMs have higher Q-factors and therefore lower thresholds. In air there are even more WGMs peaks and usually also have higher intensity than the Bragg peak. In air the WGM peaks become dominant, so it is not any more possible to distinguish the Bragg lasing from the WGM lasing without analyzing the spatially resolved spectrum.

For most applications usually single mode lasing, having only one sharp spectral line, is desirable. In the case of CLC spherical microlasers we would like to keep just the Bragg lasing and eliminate the WGM lasing. The WGMs originate from the fact that the light is trapped in the droplet as a consequence of total internal reflection on the surface of the sphere when the inside refractive index is higher than the outside index. To suppress the WGMs we just need to place the CLC microlasers in a medium with comparable or higher refractive index than CLC. In our case it was enough to transfer them from glycerol with  $n = 1.47$  to the immersion oil with the

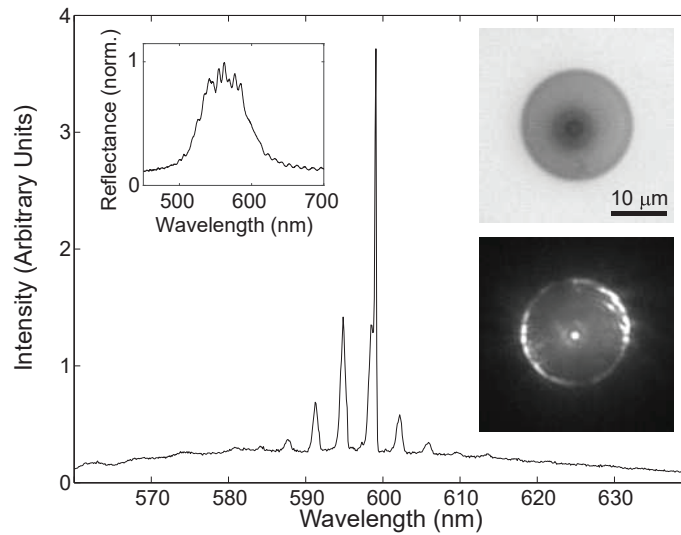


Fig. 2. The lasing spectrum from a 20  $\mu\text{m}$  diameter laser in glycerol. The broader equally spaced spectral peaks correspond to WGM lasing and the sharper highest peak corresponds to Bragg lasing. The upper left inset shows the reflectance measurement of a thin layer of undoped polymerized CLC mixture. The upper right inset shows unpolarized micrograph of the floating droplet. The bottom right inset shows lasing droplet without background illumination. The bright spot in the center corresponds to 3D Bragg lasing and the bright rim corresponds to the WGM lasing.

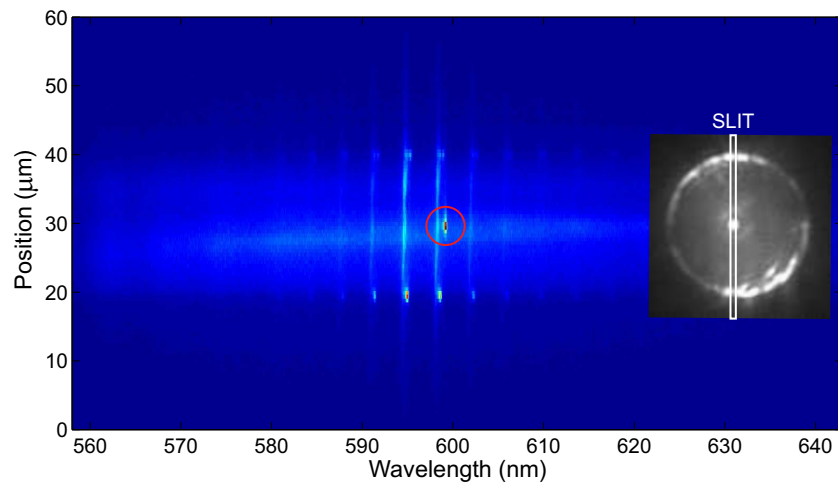


Fig. 3. Spatially resolved spectrum of the same droplet as in Fig. 2. The slit was positioned across the center of the droplet as depicted in the inset. The  $x$ -axis represents the wavelength and the  $y$ -axis represents the position along the slit. WGM lasing is seen as vertical lines across the whole diameter of the particle with maximum intensity at the edge. WGMs are easily distinguishable from the Bragg lasing that is identified as a single peak that is localized in spatial position and in wavelength (marked by a red circle).

refractive index of 1.52. Except for very large droplets, the WGMs lasing was totally suppressed and only a bright spot in the center was observed with a single sharp peak in the spectrum (Fig. 4).

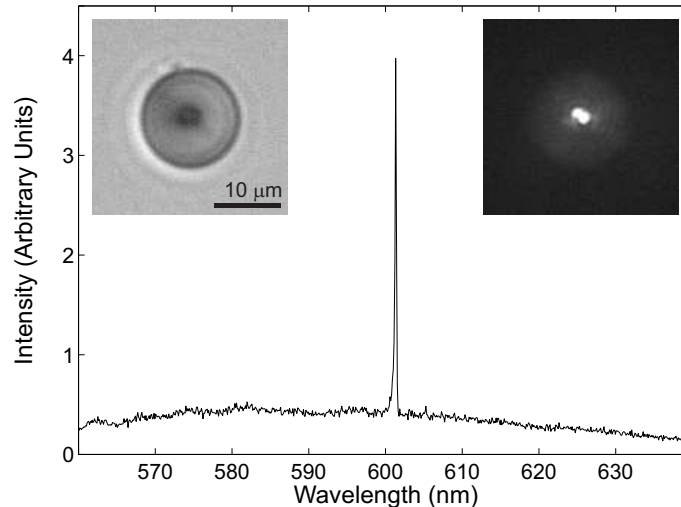


Fig. 4. The lasing spectrum from a 16  $\mu\text{m}$  diameter CLC microdroplet (inset) in high refractive index fluid ( $n = 1.52$ ). The lasing from WGMs is suppressed because of lower index difference between the interior and the exterior of the particle and only a single spectral line is observed, which corresponds to 3D Bragg lasing.

The polymerized lasers inside the immersion oil were used further to investigate their lasing properties. To test the pulse-to-pulse stability of the lasing, energies of single pulses were measured as a function of the excitation laser pulse energy (Fig. 5(a)). At lower energy the output is directly proportional to the input as can be seen as a straight line of points. At approximately  $0.6 \text{ mJ}/\text{cm}^2$  the lasing threshold is reached and the output is sharply increased. The threshold behavior also confirms that the peak we observe is indeed lasing. Above the threshold the points are more scattered meaning that for a specific input energy the energy of the output optical impulse can vary. The results can be compared to a CLC laser made of a non-polymerizable mixture. In this case the points are much more scattered (Fig. 5(b)) and there is a wide range of the input energies around the threshold where the laser may lase or may not. In polymerized lasers the region of intermittent lasing is almost negligible. Therefore, we can conclude that the pulse-to-pulse stability of the polymerizable laser is much better than of the non-polymerizable one. Also the threshold of the polymerized laser is lower than that of the one made out of the non-polymerizable mixture. But because of the different dye, dye concentration, liquid crystal used and the different diameters of the lasers, the thresholds of the two lasers can not be directly compared. With polymerization of the CLC we have achieved more stable lasing and the droplets are also mechanically stabilized.

#### 4. Conclusion

The advantages of polymerizing the CLC droplets are manifold. The most obvious advantage is that previously liquid spheres become solid and can be extracted from the original fluid and used in a dry form or embedded in other material. Further, the internal LC director configuration is preserved independent of external factors such as temperature and the pump laser and the thermal fluctuations of the LC director are quenched. This enables better pulse-to-pulse stability even at higher repetition rates than usually used with CLC lasers (10 Hz). By placing the lasers

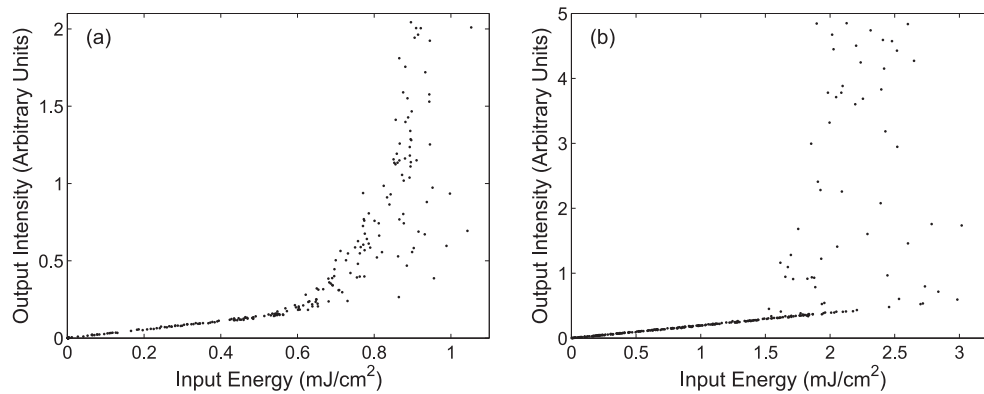


Fig. 5. (a) Output energy distribution from a single 16  $\mu\text{m}$  diameter CLC polymerized laser as the function of the input pulse energy. Each point represents a single pulse. The threshold is clearly visible at approximately 0.6  $\text{mJ}/\text{cm}^2$ . (b) The lasing characteristics for a 31  $\mu\text{m}$  microlaser made from the non-polymerizable CLC mixture shows much more scattered points. The threshold is also not so sharply defined as for the polymerized laser.

in a higher index medium, the WGMs lasing was completely inhibited and only a single spectral line remained. Alternatively, a lower index CLC could be used. However, if we would need to use the lasers in a water medium the refractive index of the CLC should be very low, lower than most of the existing LCs. Another method to suppress WGMs would be to increase the surface roughness of the droplets enabling the leakage of the circulating light. In this case the refractive index difference does not play a major role and the spherical CLC lasers having just Bragg lasing could be used in any external medium including air.

### Acknowledgements

The authors would like to thank the Slovenian Research Agency (ARRS) for grant No. J1-6732 (I.M.) and Marie Curie International Outgoing Fellowship 627274 within the 7th European Community Framework Programme (M.H.).